Smart Structures and Systems, *Vol. 27, No. 4 (2021) 679-689*
DOI: https://doi.org/10.12989/sss.2021.27.4.679

Damped forced vibration analysis of layered functionally graded thick beams with porosity

Ali Alnujaie [1], Şeref D. Akbaş*[2], Mohamed A. Eltaher [3,4] and Amr E. Assie [1,4]

[1] *Mechanical Engineering Department, Faculty of Engineering, Jazan University, P. O. Box 45142, Jazan, Kingdom of Saudi Arabia*
[2] *Department of Civil Engineering, Bursa Technical University, 16330, Bursa, Turkey*
[3] *Mechanical Engineering Department, Faculty of Engineering, King Abdulaziz University, P.O. Box 80204, Jeddah, Saudi Arabia*
[4] *Mechanical Design & Production Department, Faculty of Engineering, Zagazig University, P.O. Box 44519, Zagazig, Egypt*

(*Received June 27, 220, Revised November 8, 2020, Accepted November 27, 2020*)

Abstract. The following article presents the damped forced vibration of layered functionally graded thick beams including material porosities. In case of very thick beams, beam theories fail to satisfy boundary conditions and to predict the mechanical response accurately. So, the two-dimensional (2D) plane continuum model is exploited to model a thick functionally graded layered beam. The beam is composed from three- layers with functionally graded porous materials. The porosity is described by three different distribution models through the layer thickness. Applied forces to the functionally graded beam are assumed to be sinusoidal harmonic point load in time domain. The Kelvin–Voigt viscoelastic constitutive model is used to simulate damping effect. The governing equations are obtained by using Lagrange's equations. In frame of finite element analysis, twelve –node 2D plane element is exploited to discretize the space domain of thick beam. In the solution of the dynamic problem, the Newmark average acceleration method is used. Numerical studies illustrate effects of porosity distribution, stacking sequence, and graduation constant on the dynamic responses of layered functionally graded porous thick beams. The results show that the porosity function, stacking sequences and the damping ratio have a vital role in dynamic response of functionally graded beams. The proposed model can be used in nuclear, marine, and aerospace technologies.

Keywords: damped forced vibration; thick beam; layered functionally graded materials; porosity

1. Introduction

Since 1984, a new generation of a composite material, known as functionally graded material (FGM) whose composition created to alter continuously, is used for the first time as thermal barrier during the space-plane project in Japan, Alshorbagy *et al*. (2011). This material is capable of withstanding a surface temperature of 2000 K and a temperature gradient of 1000 K across a cross-section < 10 mm (Chen and Liew 2004). Since that, FGMs have been used in many applications such as aerospace, nuclear, optics, chemistry, biomedical, defense, automotive, energy conversion, micro/nano-electro-mechanical system (MEMS /NEMS) and atomic force microscopes.

During fabrication processes of FGMs, micro-voids and cavities are generated due to technically problems, curing or poor-quality productions. On the other hand, porosity or voids may create inside materials to provide lightweight or enhance energy-absorbing capability. Porous FGM provides unique potential for wide applications in aerospace, automotive and civil engineering. Voids are frequently presented in ceramic phase rather than metallic one. The porosity is used to measure voids percentage by determining fraction of the volume of voids on the total volume. The volume of voids over the total volume varies between 0 and 1. The porosity is very important issue in the mechanical behavior of structures because materials can lose their strength after a certain porosity ratio. Therefore, recognizing mechanical behaviors of porous FGM structural elements is significant in designs.

Recently, lots of researchers focus on this relevant topic. Wattanasakulpong and Ungbhakorn (2014) studied vibration characteristics of FGM porous beams by using differential transformation method with different kinds of elastic supports. Ebrahimi and Jafari (2016) investigated thermal vibration of FGM porous beams. Wu *et al*. (2018) performed a finite element analysis to study the free and forced vibration FGM porous beam using both Euler-Bernoulli and Timoshenko beam theories. Yang *et al*. (2018) used Chebyshev-Ritz method to study buckling and free vibration of FGM graphene reinforced porous nanocomposite. Ghayesh and Moradian (2011), Ghayesh *et al*. (2011), Ghayesh and Amabili (2012), Ghayesh (2012, 2018a, b, 2019a, b, c, d, e, f), Farokhi *et al*. (2016) investigated dynamic analysis of viscoelastic beams. Akbaş (2018a, b, c, d, e, f) examined the forced vibration analysis of FGM deep beams with porosity. Fazzolari (2018) exploited generalized beam theories to study the vibration and stability of porous FGM sandwich beams resting on elastic foundations. Jouneghani *et al*. (2018) studied analytically the structural response of porous FGM nonlocal nanobeams under hygro-thermo-mechanical loadings.

*Corresponding author, Professor,
E-mail: serefda@yahoo.com

ISSN: 1738-1584 (Print), 1738-1991 (Online)

Pegios and Hatzigeorgiou (2018) exploited the dynamic stiffness matrix for a plane system of beams by using finite element method to determine its dynamic response due to an external load harmonically varying with time. Civalek (2019) presented vibration analysis of FGM carbon nanotube plates by using singular convolution method. Ramteke *et al*. (2019, 2020) investigated effects of porosity on the eigen characteristics and static behavior of functionally graded structures. Akbaş (2014, 2015a, b, 2018g, h, 2019a) presented dynamic analysis of functionally graded beams with different mechanical cases. Akbaş (2013, 2017a, 2018a, d, f, 2019b) investigated geometrically nonlinear analysis of composite beams such as functionally graded, laminated composites by using finite element method. Akbaş (2017b, 2018b, e, 2019c, d) presented post-buckling, stability behavior of composite structures with functionally graded and laminated materials. Benahmed *et al*. (2019) investigated buckling analysis of FGM nanobeams with porosity by using higher-order shear deformation theory. Sheng and Wang (2019) studied the nonlinear forced vibration of FGM Timoshenko microbeams under thermal and damping effects including von Kármán nonlinear theory, Hamilton's principle and the modified couple stress theory. Taati and Fallah (2019) presented forced vibration of sandwich modified strain gradient microbeams with FGM core. Zhao *et al*. (2019) investigated vibration behavior of the FGM porous curved thick beam, doubly-curved panels and shells of revolution by using a semi-analytical method. Eltaher *et al* (2020a, b) studied the vibration of perforated nanobeam included piezoelectric effect. Asiri *et al*. (2020a, b), Eltaher and Akbaş (2020) presented functionally graded thick beams. Abo-bakr *et al*. (2020a, b) investigated the optimum weight of FG beam under a critical buckling load.

In accordance with literature survey and authors' knowledge, the response of Kelvin–Voigt viscoelastic thick FGM multilayered porous beam under different dynamically loads has not been considered elsewhere. So, this article tends to fill this gap. The current study illustrates transient responses of layered porous FGM thick viscoelastic beam under sinusoidal harmonic load. The paper is organized as follows: the main constitutive equations, kinematic relation, and balance equations are discussed in detailed through Section 2. The numerical procedures and discretization of the multilayer FGM porous viscoelastic thick beam structure using finite element method and Newmark implicit time integration are adopted in this section. The validation and parametric studies cto present effects of graduation parameter, geometrical and dynamical parameters on the time response of layered porous FGM thick beams are discussed in Section 3. Main remarks and conclusion points are highlighted and summarized in Section 4.

2. Problem formulation

A geometrical description of a simply supported thick beam with different functionally graded three layers including porosity under a dynamic point load $P(t)$ at midpoint is shown in Fig. 1. The dynamic point load

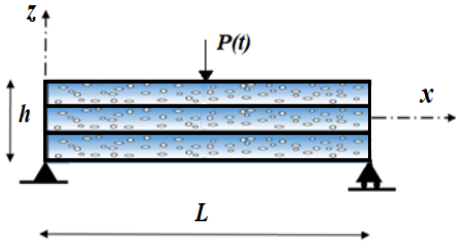

Fig. 1 Geometry of porous layered functionally graded thick beam

$P(t)$ is assumed to be sinusoidal harmonic in time domain as following

$$P(t) = P_0 \sin(\Omega t) \qquad 0 \le t \ll \infty \qquad \text{Harmonic} \tag{1}$$

where, P_0 is the amplitude of the dynamic load and Ω is its frequency.

The beam is rectangular with a length of L and a thickness of h. The functionally graded material layers are located symmetrically with mid-plane axis. The height of each layer is equal to each other. The graduation of material through each layer through transverse direction can be described by a power-law distribution as

$$E(z) = (E_T - E_B)\left[\frac{z}{h} + \frac{1}{2}\right]^n + E_B \tag{2a}$$

$$\nu(z) = (\nu_T - \nu_B)\left[\frac{z}{h} + \frac{1}{2}\right]^n + \nu_B \tag{2b}$$

$$\rho(z) = (\rho_T - \rho_B)\left[\frac{z}{h} + \frac{1}{2}\right]^n + \rho_B \tag{2c}$$

where E is Young modulus, ν is Poisson's ratio, and ρ is density. The n is the positive power exponent parameter of graduation and subscripts T and B are the top and bottom properties of the layers.

To include the effect of porosity, three different distribution models are exploited to describe the porosity in each layer. So that, equivalent mechanical and physical properties of Eq. (2) can be modified accordingly to

For Model 1:

$$E(z) = (E_T - E_B)\left[\frac{z}{h} + \frac{1}{2}\right]^n + E_B - (E_T - E_B)a \tag{3a}$$

$$\nu(z) = (\nu_T - \nu_B)\left[\frac{z}{h} + \frac{1}{2}\right]^n + \nu_B - (\nu_T - \nu_B)a \tag{3b}$$

$$\rho(z) = (\rho_T - \rho_B)\left[\frac{z}{h} + \frac{1}{2}\right]^n + \rho_B - (\rho_T - \rho_B)a \tag{3c}$$

For Model 2:

$$E(z) = (E_T - E_B)\left[\frac{z}{h} + \frac{1}{2}\right]^n + E_B - (E_T - E_B)\frac{a}{2}\left(1 - \frac{2|z|}{h}\right) \tag{4a}$$

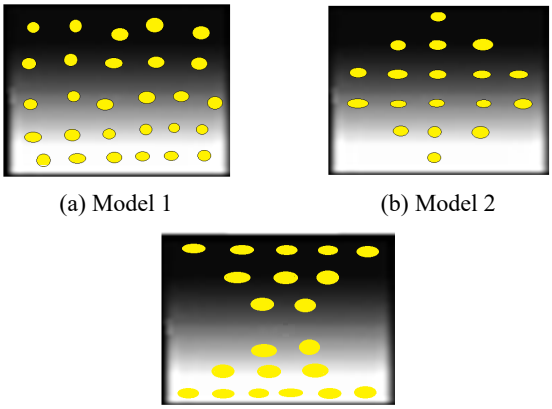

(a) Model 1 (b) Model 2

(c) Model 3

Fig. 2 Porosity models for functionally graded material

$$\nu(z) = (\nu_T - \nu_B)\left[\frac{z}{h} + \frac{1}{2}\right]^n + \nu_B - (\nu_T - \nu_B)\frac{a}{2}\left(1 - \frac{2|z|}{h}\right) \tag{4b}$$

$$\rho(z) = (\rho_T - \rho_B)\left[\frac{z}{h} + \frac{1}{2}\right]^n + \rho_B - (\rho_T - \rho_B)\frac{a}{2}\left(1 - \frac{2|z|}{h}\right) \tag{4c}$$

For Model 3:

$$E(z) = (E_T - E_B)\left[\frac{z}{h} + \frac{1}{2}\right]^n + E_B - (E_T - E_B)\frac{a}{2}\left(\frac{2|z|}{h}\right) \tag{5a}$$

$$\nu(z) = (\nu_T - \nu_B)\left[\frac{z}{h} + \frac{1}{2}\right]^n + \nu_B - (\nu_T - \nu_B)\frac{a}{2}\left(\frac{2|z|}{h}\right) \tag{5b}$$

$$\rho(z) = (\rho_T - \rho_B)\left[\frac{z}{h} + \frac{1}{2}\right]^n + \rho_B - (\rho_T - \rho_B)\frac{a}{2}\left(\frac{2|z|}{h}\right) \tag{5c}$$

where a ($a << 1$) is the volume fraction of porosities. When $a = 0$, the layer becomes Fully FGM without any porosity constituent. The distribution of the three porosity models through the layer is shown in Fig. 2. Based on the continuum mechanics, the thick beam is described by 2D plane stress problem. Therefore, the kinematic strain-displacement relations are described by

$$\begin{Bmatrix}\varepsilon_{xx}\\ \varepsilon_{zz}\\ \gamma_{xz}\end{Bmatrix} = \begin{bmatrix}\frac{\partial}{\partial x} & 0\\ 0 & \frac{\partial}{\partial z}\\ \frac{\partial}{\partial z} & \frac{\partial}{\partial x}\end{bmatrix}\begin{Bmatrix}u\\ w\end{Bmatrix} \tag{6a}$$

$$\{\varepsilon\} = [B]\{d\} \tag{6b}$$

in which u, w are the displacements in x and z directions, respectively. ε_{xx} and ε_{zz} are the normal in-plane strains, and γ_{xz} is the shear in-plane strain. The constitutive stress-strain equation, in a case of FGM layer, can be represented as

$$\begin{Bmatrix}\sigma_{xx}\\ \sigma_{zz}\\ \sigma_{xz}\end{Bmatrix} = \begin{bmatrix}Q_{11}(z) & Q_{12}(z) & 0\\ Q_{12}(z) & Q_{22}(z) & 0\\ 0 & 0 & Q_{33}(z)\end{bmatrix}\begin{Bmatrix}\varepsilon_{xx}\\ \varepsilon_{zz}\\ \gamma_{xz}\end{Bmatrix} \tag{7a}$$

$$\{\sigma\} = [Q]\{\varepsilon\} \tag{7b}$$

where coefficients of the stiffness can be described as functions of elasticity and Poisson's ratio as following

$$\begin{aligned} Q_{11}(z) = Q_{22}(z) &= \frac{E(z)}{1 - [v(z)]^2},\\ Q_{33}(z) &= \frac{E(z)}{2\,[1 + v(z)]};\\ Q_{12}(z) &= \frac{v(z)E(z)}{1 - [v(z)]^2} \end{aligned} \tag{8}$$

To consider the internal damping of the proposed material, the Kelvin–Voigt viscoelastic model is exploited. Therefore, the constitutive equations of a FGM layer is adopted to

$$\begin{Bmatrix}\sigma_{xx}\\ \sigma_{zz}\\ \sigma_{xz}\end{Bmatrix} = \begin{bmatrix}Q_{11}(z) & Q_{12}(z) & 0\\ Q_{12}(z) & Q_{22}(z) & 0\\ 0 & 0 & Q_{33}(z)\end{bmatrix}\begin{Bmatrix}\varepsilon_{xx}\\ \varepsilon_{zz}\\ \gamma_{xz}\end{Bmatrix} + \eta(z\begin{bmatrix}Q_{11}(z) & Q_{12}(z) & 0\\ Q_{12}(z) & Q_{22}(z) & 0\\ 0 & 0 & Q_{33}(z)\end{bmatrix}\begin{Bmatrix}\frac{\partial \varepsilon_{xx}}{\partial t}\\ \frac{\partial \varepsilon_{zz}}{\partial t}\\ \frac{\partial \gamma_{xz}}{\partial t}\end{Bmatrix} \tag{9a}$$

$$\{\sigma\} = [C]\{\varepsilon\} + [D]\{\dot{\varepsilon}\} \tag{9b}$$

where, η is the damping ratio

$$\eta = \frac{c}{E} \tag{10}$$

where, c is the damping coefficient. Strain energy (U_i), kinetic energy (T), dissipation function (R) and potential energy of the external loads (U_e) are presented as follows

$$U_i = \frac{1}{2}\{d\}^T\left(\int_V [B]^T[C][B]\right)\{d\}dV \tag{11}$$

$$T = \frac{1}{2}\{\dot{d}\}^T\left(\int_V \rho(z)\right)\{\dot{d}\}dV \tag{12}$$

$$R = \frac{1}{2}\{\dot{d}\}^T\left(\int_V [B]^T[D][B]\right)\{\dot{d}\}dV \tag{13}$$

$$U_e = -P(t)w(x_p, t) \tag{14}$$

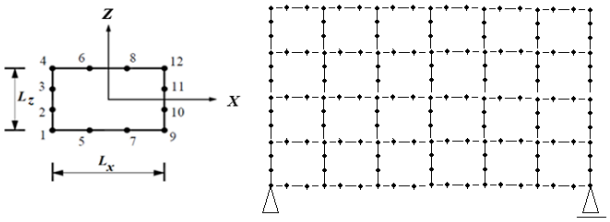

Fig. 3 Twelve–node 2D plane finite element model

in which $\{\dot{d}\}$ is the velocity vector, x_p is the coordinate of the applied load. The Lagrangian functional of the problem is presented as follows

$$I = T - (U_i + U_e) \tag{15}$$

The proposed model is solved by using finite element method with Twelve-node 2D-plane element model, as illustrated in Fig. 3.
where L_x and L_z are element lengths in X and Z directions respectively. The displacement vector for Twelve-node plane element is expressed as

$$\{d\} = \begin{bmatrix} \emptyset & 0 \\ 0 & \emptyset \end{bmatrix} \{d_n\} \tag{16a}$$

$$[\emptyset] = [\emptyset_1\ \emptyset_2\ ....\emptyset_{12}] \tag{16b}$$

$$\{d\} = \begin{Bmatrix} u \\ w \end{Bmatrix} \tag{16c}$$

where $\{d_n\}$ is the nodal displacement vector and its components are u_i and w_i are the displacement components for any node, i. The displacement of any generic point within the element can be represented by its nodal values and corresponding functions as

$$\{d_n\} = \{u_1\ u_2\ ..u_{12}\ w_1\ w_2\ .\ .w_{12}\}^T \tag{17}$$

$$u = \sum_{i=1}^{12} u_i \emptyset_i \tag{18}$$

$$w = \sum_{i=1}^{12} w_i \emptyset_i \tag{19}$$

where $\emptyset_i$ is the nonlinear interpolation shape functions, which were developed by Akbaş (2018c).

Substituting Eqs. (18), (19), into the energy Eqs. (11), (14) and Lagrangian functional, and then Lagrange's equations are presented as following

$$\begin{aligned} &\frac{\partial \mathrm{I}}{\partial \mathrm{q}_\mathrm{k}^{(\mathrm{e})}} - \frac{\partial}{\partial \mathrm{t}} \frac{\partial \mathrm{I}}{\partial \dot{\mathrm{q}}_\mathrm{k}^{(\mathrm{e})}} + \mathrm{Q}_{\mathrm{D_k}} = 0, \\ &\mathrm{Q}_{\mathrm{D_k}} = -\frac{\partial \mathrm{R}}{\partial \dot{\mathrm{q}}_\mathrm{k}^{(\mathrm{e})}}, \qquad k = 1, 2, \ldots, 12 \end{aligned} \tag{20}$$

where $\mathrm{Q}_{\mathrm{D_k}}$ is generalized damping load. After using the Lagrange procedure, the dynamic equilibrium equation is written as follows

$$[K]\{d_n\} + [C]\{\dot{d}_n\} + [M]\{\ddot{d}_n\} = \{F\} \tag{21}$$

where $[K]$, $[C]$, $[M]$, $\{F\}$, $\{d_n\}$, $\{\dot{d}_n\}$ and $\{\ddot{d}_n\}$ are the stiffness matrix, damping matrix, mass matrix, load vector, displacement vector, velocity vector and acceleration vector per element, respectively. The expansions of finite element matrices are represented as

$$[K] = b \int_A [H]^T [Q][H] dA \tag{22a}$$

$$[C] = b \int_A \eta [H]^T [Q][H] dA \tag{22b}$$

$$[M] = b \int_A \rho(z) [\emptyset]^T [\emptyset] dA \tag{22c}$$

$$\{F\} = \int_\Gamma \{\delta d_n\}^T [\emptyset]^T P(t) d\Gamma \tag{22d}$$

where

$$[H] = \begin{bmatrix} \dfrac{\partial}{\partial X} & 0 \\ 0 & \dfrac{\partial}{\partial Z} \\ \dfrac{\partial}{\partial Z} & \dfrac{\partial}{\partial X} \end{bmatrix} [\emptyset] \tag{23}$$

The governing equation of motions of the whole beam is obtained from the assembly of Eq. (21) and then is solved numerically by using implicit Newmark average acceleration $(\alpha = 0.5\,, \beta = 0.25)$ scheme in the time domain. Through this procedure, the dynamic problem is transferred to a system of static problem in each step as following

$$[\overline{\boldsymbol{K}}(t)]\{\boldsymbol{d_m}\}_{j+1} = \{\overline{\boldsymbol{F}}(t)\} \tag{24}$$

in which

$$[\overline{\boldsymbol{K}}(t)] = [\boldsymbol{K_m}] + \frac{[\boldsymbol{M_m}]}{\beta \Delta t^2} + \frac{[\boldsymbol{C_m}]\alpha}{\beta \Delta t} \tag{25a}$$

$$\begin{aligned} \{\overline{\boldsymbol{F}}(t)\} = {} & \{\boldsymbol{F_m}(t)\}_{j+1} + B_1 \{\boldsymbol{d_m}\}_j \\ & + B_2 \{\dot{\boldsymbol{d}}_\boldsymbol{m}\}_j + B_3 \{\ddot{\boldsymbol{d}}_\boldsymbol{m}\}_j \end{aligned} \tag{25b}$$

where

$$\begin{aligned} B_1 &= \frac{[\boldsymbol{M_m}]}{\beta \Delta t^2} + \frac{[\boldsymbol{C_m}]\alpha}{\beta \Delta t}, \\ B_2 &= \frac{[\boldsymbol{M_m}]}{\beta \Delta t} + [\boldsymbol{C_m}] \left(\frac{\alpha}{\beta} - 1 \right), \\ B_3 &= [\boldsymbol{M_m}] \left(\frac{1}{2\beta} - 1 \right) + [\boldsymbol{C_m}] \left(\frac{\alpha}{2\beta} - 1 \right) \end{aligned} \tag{26}$$

After evaluating $\{\boldsymbol{d_m}\}_{j+1}$ at a time $t_{j+1} = t_j + \Delta t$, the acceleration and velocity vectors can be evaluated by

$$\{\ddot{\boldsymbol{d}}_{\boldsymbol{m}}\}_{j+1} = \frac{1}{\beta\Delta t^2}\left(\{\boldsymbol{d}_{\boldsymbol{m}}\}_{j+1} - \{\boldsymbol{d}_{\boldsymbol{m}}\}_j\right) - \frac{[\boldsymbol{M}_{\boldsymbol{m}}]}{\beta\Delta t}\{\dot{\boldsymbol{d}}_{\boldsymbol{m}}\}_j - \left(\frac{\alpha}{2\beta} - 1\right)\{\ddot{\boldsymbol{d}}_{\boldsymbol{m}}\}_j \quad (27a)$$

$$\{\dot{\boldsymbol{d}}_{\boldsymbol{m}}\}_{j+1} = \{\dot{\boldsymbol{d}}_{\boldsymbol{m}}\}_j + \Delta t\,(1-\alpha)\{\ddot{\boldsymbol{d}}_{\boldsymbol{m}}\}_j + \Delta t\,\alpha\,\{\ddot{\boldsymbol{d}}_{\boldsymbol{m}}\}_{j+1} \quad (27b)$$

where $[\boldsymbol{K}_{\boldsymbol{m}}]$, $[\boldsymbol{C}_{\boldsymbol{m}}]$, $[\boldsymbol{M}_{\boldsymbol{m}}]$, $\{\boldsymbol{F}_{\boldsymbol{m}}\}$, $\{\boldsymbol{d}_{\boldsymbol{m}}\}$, $\{\dot{\boldsymbol{d}}_{\boldsymbol{m}}\}$ and $\{\ddot{\boldsymbol{d}}_{\boldsymbol{m}}\}$ are the stiffness matrix, damping matrix, mass matrix, load vector, displacement vector, velocity vector and acceleration vector per assembly, respectively.

3. Numerical results

In this section, effects of graduation parameter, geometrical and stacking sequence of layers and damping ratio on the time response of simply supported layered FGM thick beam are discussed and presented in detail. The materials of FGM layers are considered as Aluminium (Al; E = 70 GPa, ν = 0.3, ρ = 2702 kg/m^3) and Zirconia (E = 151 GPa, ν = 0.3, ρ = 3000 kg/m^3). Through the results, sinusoidal harmonic loads, two different stacking sequences of layers as shown in Fig. 4 and three different porosity distribution models are proposed. The dimensions of the FGM thick beam are considered as follows: b = 0.15 m (beam width), h = 0.15 m and L = 0.6 m (L/h = 4) in the numerical analysis. The height of each layer is equal. The five-point Gauss rule is used to calculate integrations. In the numerical process, the number 0f elements is taken as 30 in both X and Z directions, where the dynamic response converges. The damping ratio of Aluminium is considered as $\eta_{Al} = 0.001$ and the damping ratio of Zirconia is selected as according to multiples of Aluminium value, such as $\eta_{zr}/\eta_{Al} = 1$. The damping ratio of each layer graded through height direction according to Eq. (10).

This section is divided into two subsections; the first one presents the model validation. The 2nd subsection is devoted to numerical results and parametric studies to present the effect of graduation distributions, stacking sequences, porosity function, porosity percentage and the damping ratio on the fundamental frequencies and dynamic response of layered FGM thick beams.

3.1 Problem validation

To validate the present study, a comparison with the obtained results using ANSYS package is performed. The maximum vertical displacement of a fully Aluminum beam is obtained and compared with ANSYS under load of Eq. (1) for L/h = 5, P_0 = 1000 KN and Ω = 2 rad/s in Fig. 5. It is seen from this figure that: results of the current study are approximately identical with those of ANSYS.

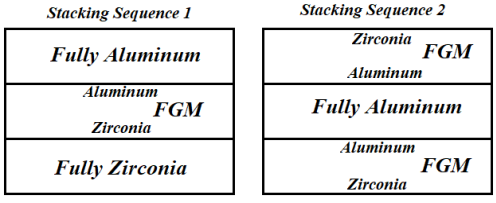

Fig. 4 Stacking sequence distributions through the beam thickness

In another comparison study, fundamental frequencies of a simply supported FGM porous beam are compared for different porosity and FGM parameters in Table 1 with results of Ebrahimi and Jafari (2016). The fundamental frequencies are presented as dimensionless values ($\bar{\omega} = \omega\sqrt{\rho_B L^4/E_B\,h^2}$). The fundamental frequencies are obtained from the eigenvalue solution of the assembled equation. As seen from Table 1, the presented results are close to the published work.

3.2 Parametric studies

Effect of porosity model, porosity factor (a), graduation parameter (n), stacking sequence and damping ratio for sinusoidal harmonic load on the dynamic response of FGM thick beam are investigated in detail through these subsections:

a) Results of the stacking sequence 1

Fig. 6 illustrates the time response at the mid-point of thick beam (vertical displacement, w) with *the stacking sequence 1*. including porosity distribution with model 1, under the harmonic load with the following properties: frequency Ω = 2 rad/s and P_0 = 1000 KN. The beam is assumed to be damped with damping ratio η = 0.001. As shown, by increasing the graduation distribution parameter (n), the amplitude of displacement response decreases.

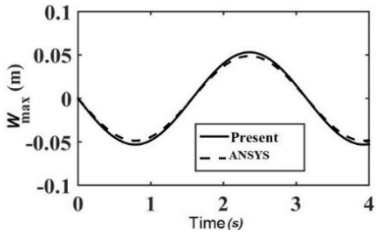

Fig. 5 Comparison study: Time responses of the fully Aluminium beam for L/h = 5, P_0 = 1000 KN and Ω = 2 rad/s

Table 1 Dimensionless fundamental frequencies of porous FGM beam (L/h = 20)

Porosity models	a	n = 0.5		n = 2	
		Present	Ebrahimi and Jafari (2016)	Present	Ebrahimi and Jafari (2016)
Model 1	0	4.52911	4.51585	3.5661	3.55529
	0.1	4.5953	4.58213	3.5202	3.50825
	0.2	4.6761	4.66783	3.4606	3.44947
Model 2	0	4.5391	4.51585	3.5643	3.55529
	0.1	4.6182	4.60304	3.5912	3.58170
	0.2	4.7184	4.70024	3.6381	3.61002

However, increasing the porosity parameter (a) accompanying by reduction in stiffness, tends to increase the amplitude of response. As illustrated for all cases the displacement response for a porosity a = 0.3 is greater than the full beam without porosity (a = 0). It is observed that, the porosity has no effect on the time period of oscillation. Since, in the current analysis, the damping ratio is very close to zero and initial conditions are assumed to be zero,

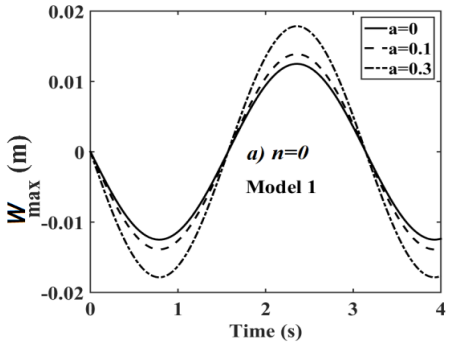

(a) for n = 0

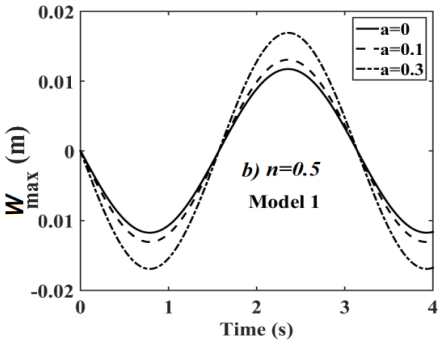

(b) for n = 0.5

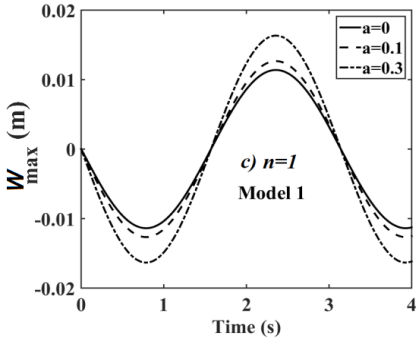

(c) for n = 1

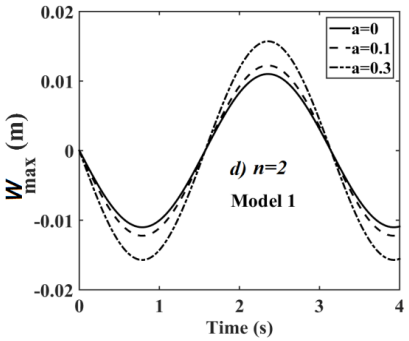

(d) for n = 2

Fig. 6 Time responses of thick beam with stacking sequences 1 in model 1 with different porosity parameters

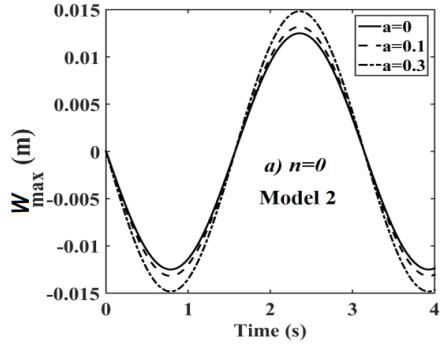

(a) for n = 0

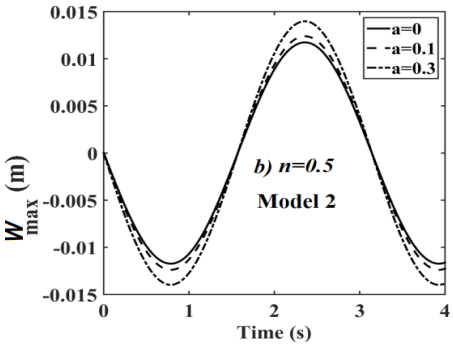

(b) for n = 0.5

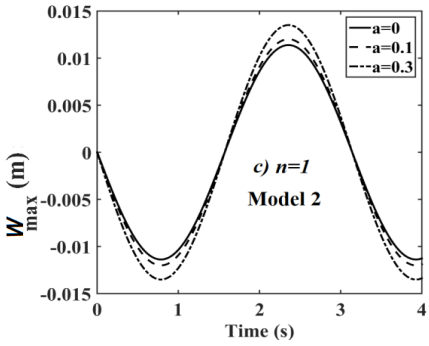

(c) for n = 1

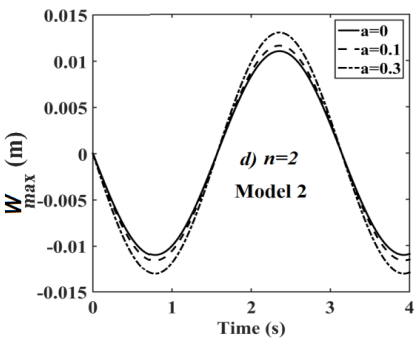

(d) for n = 2

Fig. 7 Time responses of thick beam with stacking sequences 1 in model 2 with different porosity parameters

therefore the transient response of the system is equivalent to steady state response.

With the same previous stacking sequence and other conditions except a model of porosity, the time response for porosity model 2 is illustrated in Fig. 7. The graduation parameter has the inverse effect of porosity parameter on the time response of FGM thick beams. As illustrated the amplitude of displacement decrease with increasing the

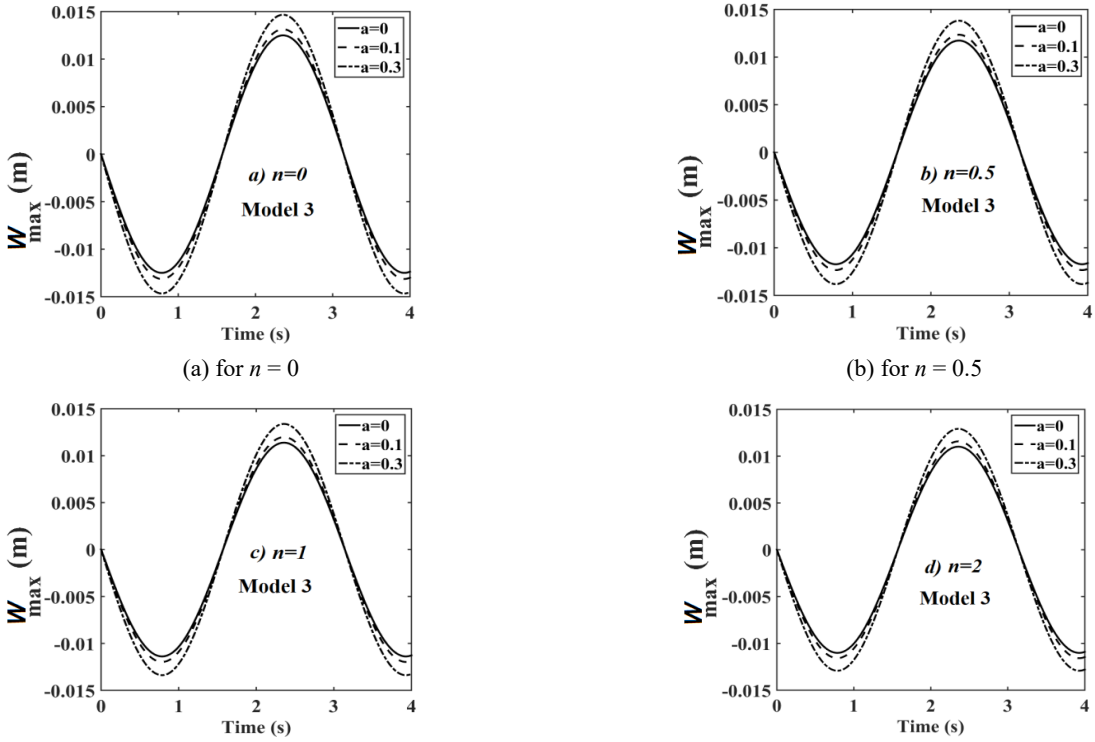

(a) for n = 0 (b) for n = 0.5

(c) for n = 1 (d) for n = 2

Fig. 8 Time responses of thick beam with stacking sequences 1 in model 3 with different porosity parameters

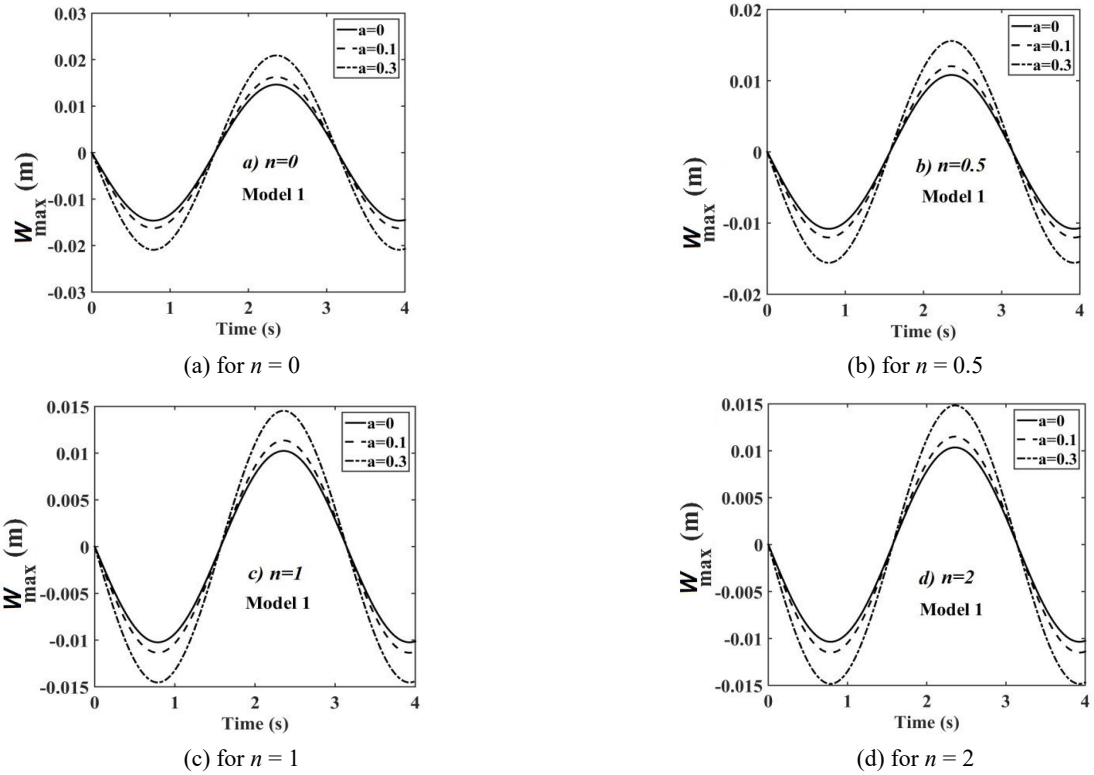

(a) for n = 0 (b) for n = 0.5

(c) for n = 1 (d) for n = 2

Fig. 9 Time responses of thick beam with stacking sequences 2 in model 1 with different porosity parameters

graduation parameter, and increasing with increasing of porosity parameter. By comparing Fig. 6 by Fig. 7, it is noted that, the effect of the model 1 of porosity is more significant on the time response rather than that of model 2.

The effect of model 3 of porosity on the time response of thick beam with the previous configuration and subjected to harmonic sinusoidal load is shown in Fig. 8. As presented, all phenomena observed in this mode are consistent with model 1 and model 2 of porosity. By comparing the three Figs. 6-8, it is noted that: model 1 has the highest effect on the time response rather that the other two models. It is also observed that, the model 2 and model 3 has equal effects on the dynamic response of proposed structure.

b) Results of the stacking sequence 2

The time responses of the mid-point deflection of thick beam with the stacking sequence 2 under the sinusoidal harmonic point load with various graduation parameter and porosity percentage for model 1 are presented in Fig. 9. A shown, the deflection amplitude is decreased significant with increasing the graduation parameter from 0 to 1. However, increasing a graduation parameter from 1 to 2, no significant effect has been observed on the amplitude deflection. It is observed by increasing the porosity percentage for a specified case from 0 to 0.3, the deflection increased by 50%. So, the porosity tends to soften the rigidity of structure. The porosity and graduation parameters have no effect on the time period of oscillation.

Fig. 10 illustrates the effect of model 2 of porosity on dynamic response for FGM structure at different graduation and porosity percentage. As predicted from pervious case, the graduation parameter has a significant effect on the deflection through $n = 0$ to $n = 1$, and has no effect on the deflection when $n > 1$. The porosity percentage in this model has a little effect on the deflection comparable to model 1.

The dynamic responses for the mid-point deflection of thick beam under harmonic sinusoidal load and different graduation parameter and porosity percentage for model 3 of porosity are illustrated in Fig. 11. By comparing Fig. 10 with Fig. 11, it is noticed that all phenomena observed in the previous configuration (porosity models) are the same as in the current case. Thus, it can conclude that, the model 2 and model 3 of porosity have the same effect on the dynamic response of thick beam with stacking sequence 2. It is also noticed from figures that the stacking sequence 1 is more rigid than the stacking sequence 2. The stacking sequence has important role on the effects of the porosity on the dynamic behavior of the multilayered FG beams.

c) Effect of damping ratio (η)

Effects of the damping ratios on the steady state dynamic responses of thick beam under sinusoidal harmonic load are plotted in Fig. 12 for $a = 0.3$, $n = 1$ and with the stacking sequence 1. As shown in this figure, by increasing the damping ratio, the harmonic displacement amplitude is decreased, and time period is increased. The effect of damping ratio in the region, 0.001 to 0.1 on the dynamic response is a little bit significant. However, by increasing the damping from 0.1 to 0.5 significant influences on the amplitude and time period have been predicted.

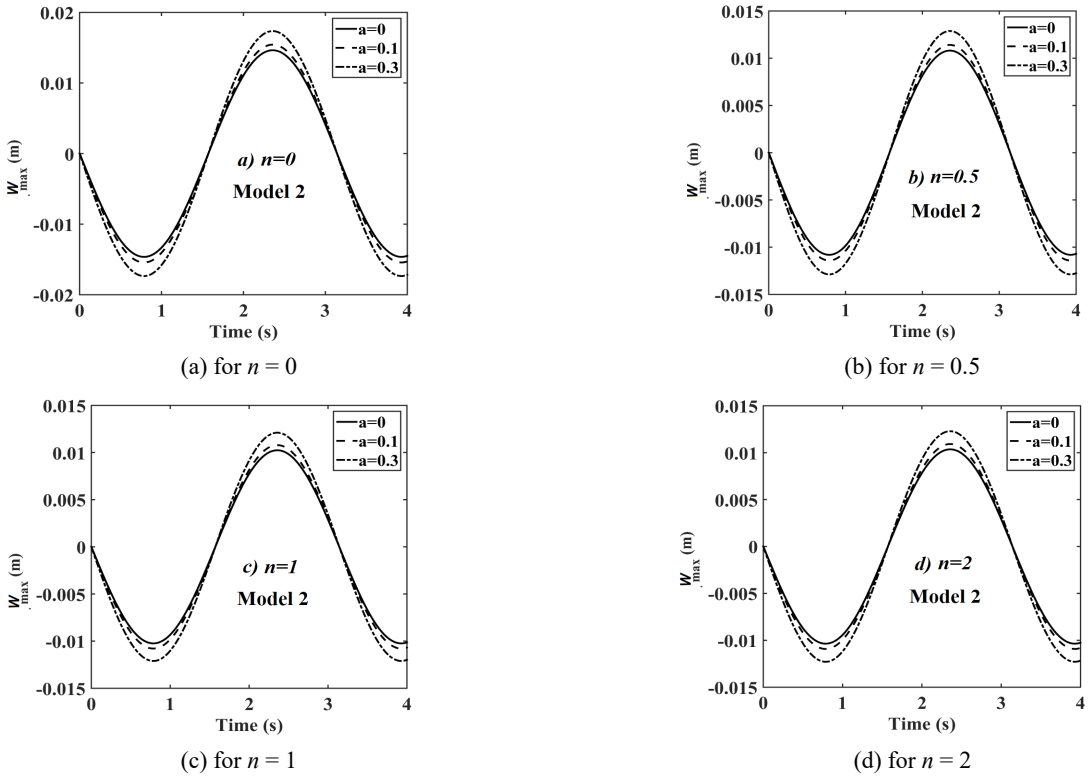

(a) for $n = 0$ (b) for $n = 0.5$

(c) for $n = 1$ (d) for $n = 2$

Fig. 10 Time responses of thick beam with stacking sequences 2 in model 2 with different porosity parameters

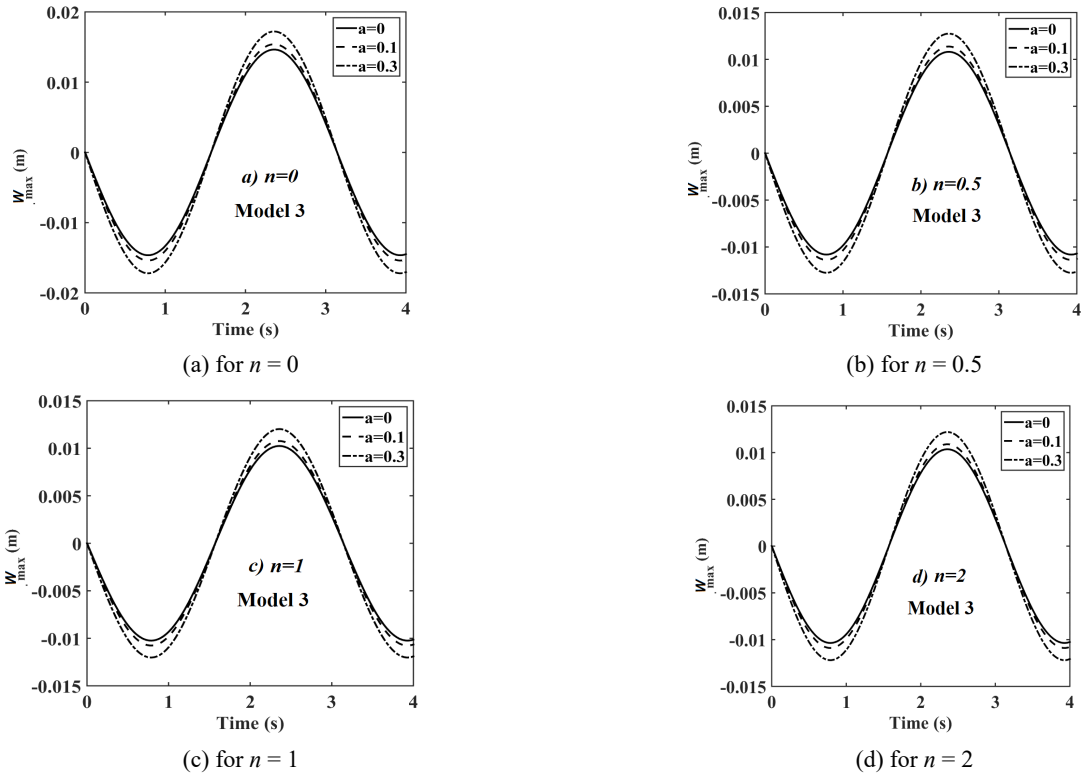

(a) for $n = 0$ (b) for $n = 0.5$

(c) for $n = 1$ (d) for $n = 2$

Fig. 11 Time responses of thick beam with stacking sequences 2 in model 3 with different porosity parameters

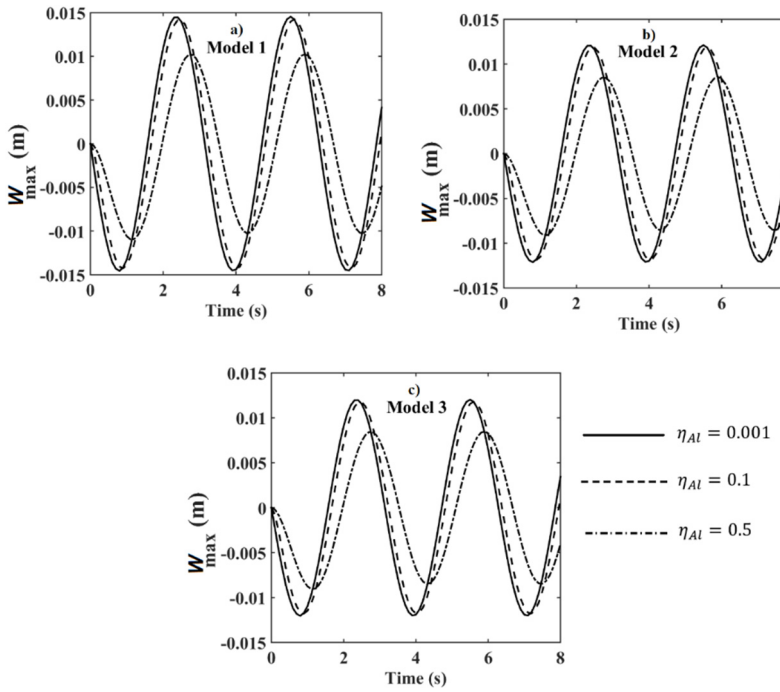

Fig. 12 Time responses of thick beam with stacking sequences 1 for Sinusoidal Harmonic Load with different damping ratios for (a) model 1; (b) model 2; and (c) model 3

4. Conclusions

The vibration responses of porous layered FGM thick beam with various stacking sequences and damping ratios under sinusoidal harmonic load have been investigated in detail through this article. The kinematic assumption and constitutive equation of beam structure is assumed to be 2D with plane stress constitutive equation, to consider the shear effect of beam thickness effectively without using beam theories. Twelve-node 2D-plane finite element is used to discretize the spatial beam domain. The Kelvin–Voigt viscoelastic constitutive model is used to consider present

the material damping effect. The governing equations are obtained by using Lagrange's equations. Newmark time integration is assumed to transform the dynamic problem to a system of static problems at each time step. The comparison study shows the accuracy of proposed model. The current model can be used in nuclear, marine, and aerospace applications. Several conclusions can be deduced from parametric studies as follows:

- The porosity and graduation parameters have a very important role on the amplitude of dynamic displacements of the FGM thick beam.
- By increasing the graduation distribution parameter (n), the amplitude of displacement response decreases.
- The stacking sequence has important role on the effects of the porosity on the dynamic behavior of the multilayer FGM beams.
- The amplitude of displacement decreases with increasing the graduation parameter and increasing with increasing of porosity parameter.
- The graduation parameter has the inverse effect of porosity parameter on dynamic results of FGM thick beams.
- The dynamic responses of thick FGM beams vary greatly in different porosity distribution models.
- Porosity distribution model 1 has the highest effect on the dynamic responses rather than that of the other two models.
- The porosity has no effect on the time period of oscillation.
- It is noticed from figures that the stacking sequence 1 is more rigid than the stacking sequence 2.
- The effect of damping ratio in the region, 0.001 to 0.1 on the dynamic response is a little bit significant. However, by increasing the damping from 0.1 to 0.5 significant influences on the amplitude and time period have been predicted.
- With suitable designing of stacking sequence and determining the graduation parameters, the porosity effects can be reduced.

Acknowledgments

The project was funded by Deanship of Scientific Research (DSR) at Jazan University, Jazan, Kingdom of Saudi Arabia under grant no. W41-045. The authors acknowledge with thanks DSR for technical and financial support.

References

Abo-bakr, R.M., Abo-bakr, H.M., Mohamed, S.A. and Eltaher, M.A. (2020a), "Optimal Weight for Buckling of FG Beam under Variable Axial Load using Pareto Optimality", *Compos. Struct.*, 113193. https://doi.org/10.1016/j.compstruct.2020.113193

Abo-Bakr, H.M., Abo-Bakr, R.M., Mohamed, S.A. and Eltaher, M.A. (2020b), "Weight optimization of axially functionally graded microbeams under buckling and vibration behaviors", *Mech. Based Des. Struct. Mach.*, 1-22. https://doi.org/10.1080/15397734.2020.1838298

Akbaş, Ş.D. (2013), "Geometrically nonlinear static analysis of edge cracked Timoshenko beams composed of functionally graded material", *Mathe. Problems Eng.*, 2013. https://doi.org/10.1155/2013/871815

Akbaş, Ş.D. (2014), "Free vibration of axially functionally graded beams in thermal environment", *Int. J. Eng. Appl. Sci.*, **6**(3), 37-51. https://doi.org/10.24107/ijeas.251224

Akbaş, Ş.D. (2015a), "Wave propagation of a functionally graded beam in thermal environments", *Steel Compos. Struct.*, *Int. J.*, **19**(6), 1421-1447. https://doi.org/10.12989/scs.2015.19.6.1421

Akbaş, Ş.D. (2015b), "Free vibration and bending of functionally graded beams resting on elastic foundation", *Res. Eng. Struct. Mater.*, **1**(1), 25-37. http://dx.doi.org/10.17515/resm2015.03st0107

Akbaş, Ş.D. (2017a), "Nonlinear static analysis of functionally graded porous beams under thermal effect", *Coupl. Syst. Mech.*, *Int. J.*, **6**(4), 399-415. https://doi.org/10.12989/csm.2017.6.4.399

Akbaş, Ş.D. (2017b), "Stability of a non-homogenous porous plate by using generalized differantial quadrature method", *Int. J. Eng. Appl. Sci.*, **9**(2), 147-155. https://doi.org/10.24107/ijeas.322375

Akbaş, Ş.D. (2018a), "Nonlinear thermal displacements of laminated composite beams", *Coupl. Syst. Mech.*, *Int. J.*, **7**(6), 691-705. https://doi.org/10.12989/csm.2018.7.6.691

Akbaş, Ş.D. (2018b), "Post-buckling responses of a laminated composite beam", *Steel Compos. Struct.*, *Int. J.*, **26**(6), 733-743. https://doi.org/10.12989/scs.2018.26.6.733

Akbaş, Ş.D. (2018c), "Forced vibration analysis of functionally graded porous deep beams", *Compos. Struct.*, **186**, 293-302. https://doi.org/10.1016/j.compstruct.2017.12.013

Akbaş, Ş.D. (2018d), "Geometrically nonlinear analysis of functionally graded porous beams", *Wind Struct.*, *Int. J.*, **27**(1), 59-70. https://doi.org/10.12989/was.2018.27.1.059

Akbaş, Ş.D. (2018e), "Thermal post-buckling analysis of a laminated composite beam", *Struct. Eng. Mech.*, *Int. J.*, **67**(4), 337-346. http://dx.doi.org/10.12989/sem.2018.67.4.337

Akbaş, Ş.D. (2018f), "Geometrically nonlinear analysis of a laminated composite beam", *Struct. Eng. Mech.*, *Int. J.*, **66**(1), 27-36. http://dx.doi.org/10.12989/sem.2018.66.1.027

Akbaş, Ş.D. (2018g), "Investigation on free and forced vibration of a bi-material composite beam", *J. Polytech.-Politeknik Dergisi*, **21**(1), 65-73. http://dx.doi.org/10.2339/politeknik.386841

Akbaş, Ş.D. (2018h), "Investigation of static and vibration behaviors of a functionally graded orthotropic beam", *Balıkesir Üniversitesi Fen Bilimleri Enstitüsü Dergisi*, 1-14. https://doi.org/10.25092/baunfbed.343227

Akbaş, Ş.D. (2019a), "Forced vibration analysis of functionally graded sandwich deep beams", *Coupl. Syst. Mech.*, *Int. J.*, **8**(3), 259-271. http://dx.doi.org/10.12989/csm.2019.8.3.259

Akbaş, Ş.D. (2019b), "Hygro-thermal nonlinear analysis of a functionally graded beam", *J. Appl. Computat. Mech.*, **5**(2), 477-485. http://dx.doi.org/10.22055/JACM.2018.26819.1360

Akbaş, Ş.D. (2019c), "Hygrothermal post-buckling analysis of laminated composite beams", *Int. J. Appl. Mech.*, **11**(1), 1950009. https://doi.org/10.1142/S1758825119500091

Akbaş, Ş.D. (2019d), "Hygro-thermal post-buckling analysis of a functionally graded beam", *Coupl. Syst. Mech.*, *Int. J.*, **8**(5), 459-471. http://dx.doi.org/10.12989/csm.2019.8.5.459

Alshorbagy, A.E., Eltaher, M.A. and Mahmoud, F.F. (2011), "Free vibration characteristics of a functionally graded beam by finite element method", *Appl. Mathe. Modell.*, **35**(1), 412-425. https://doi.org/10.1016/j.apm.2010.07.006

Asiri, S.A., Akbas, Ş.D. and Eltaher, M.A. (2020a), "Damped dynamic responses of a layered functionally graded thick beam under a pulse load", *Struct. Eng. Mech.*, *Int. J.*, **75**(6), 713-722.

https://doi.org/10.12989/sem.2020.75.6.713
Asiri, S.A., Akbas, S.D. and Eltaher, M.A. (2020b), "Dynamic Analysis of Layered Functionally Graded Viscoelastic Deep Beams with Different Boundary Conditions due to a Pulse Load", *Int. J. Appl. Mech.*, **12**(5), 2050055. https://doi.org/10.1142/S1758825120500556
Benahmed, A., Fahsi, B., Benzair, A., Zidour, M., Bourada, F. and Tounsi, A. (2019), "Critical buckling of functionally graded nanoscale beam with porosities using nonlocal higher-order shear deformation", *Struct. Eng. Mech., Int. J.*, **69**(4), 457-466. https://doi.org/10.12989/sem.2019.69.4.457
Chen, X.L. and Liew, K.M. (2004), "Buckling of rectangular functionally graded material plates subjected to nonlinearly distributed in-plane edge loads", *Smart Mater. Struct.*, **13**(6), 1430. https://doi.org/10.1088/0964-1726/13/6/014
Civalek, Ö. (2019), "Vibration of functionally graded carbon nanotube reinforced quadrilateral plates using geometric transformation discrete singular convolution method", *Int. J. Numer Methods Eng.*, **11**, 205-216. https://doi.org/10.1002/nme.6254
Ebrahimi, F. and Jafari, A. (2016), "A higher-order thermomechanical vibration analysis of temperature-dependent FGM beams with porosities", *J. Eng.*, 2016. http://dx.doi.org/10.1155/2016/9561504
Eltaher, M.A. and Akbas, Ş.D. (2020), "Transient response of 2D functionally graded beam structure", *Struct. Eng. Mech., Int. J.*, **75**(3), 357-367. https://doi.org/10.12989/sem.2020.75.3.357
Eltaher, M.A., Omar, F.A., Abdraboh, A.M., Abdalla, W.S. and Alshorbagy, A.E. (2020a), "Mechanical behaviors of piezoelectric nonlocal nanobeam with cutouts", *Smart Struct. Syst., Int. J.*, **25**(2), 219-228. https://doi.org/10.12989/sss.2020.25.2.219
Eltaher, M.A. and Mohamed, N.A. (2020b), "Vibration of nonlocal perforated nanobeams with general boundary conditions", *Smart Struct. Syst., Int. J.*, **25**(4), 501-514. https://doi.org/10.12989/sss.2020.25.4.501
Farokhi, H., Ghayesh, M.H. and Hussain, S. (2016), "Three-dimensional nonlinear global dynamics of axially moving viscoelastic beams", *J. Vib. Acoust.*, **138**(1). https://doi.org/10.1115/1.4031600
Fazzolari, F.A. (2018), "Generalized exponential, polynomial and trigonometric theories for vibration and stability analysis of porous FG sandwich beams resting on elastic foundations", *Compos. Part B: Eng.*, **136**, 254-271. https://doi.org/10.1016/j.compositesb.2017.10.022
Ghayesh, M.H. (2012), "Nonlinear dynamic response of a simply-supported Kelvin–Voigt viscoelastic beam, additionally supported by a nonlinear spring", *Nonlinear Anal.: Real World Applic.*, **13**(3), 1319-1333. https://doi.org/10.1016/j.nonrwa.2011.10.009
Ghayesh, M.H. (2018a), "Nonlinear vibration analysis of axially functionally graded shear-deformable tapered beams", *Appl. Mathe. Modell.*, **59**, 583-596. https://doi.org/10.1016/j.apm.2018.02.017
Ghayesh, M.H. (2018b), "Dynamics of functionally graded viscoelastic microbeams", *Int. J. Eng. Sci.*, **124**, 115-131. https://doi.org/10.1016/j.ijengsci.2017.11.004
Ghayesh, M.H. (2019a), "Viscoelastic mechanics of Timoshenko functionally graded imperfect microbeams", *Compos. Struct.*, **225**, 110974. https://doi.org/10.1016/j.compstruct.2019.110974
Ghayesh, M.H. (2019b), "Mechanics of viscoelastic functionally graded microcantilevers", *Eur. J. Mech.-A/Solids*, **73**, 492-499. https://doi.org/10.1016/j.euromechsol.2018.09.001
Ghayesh, M.H. (2019c), "Asymmetric viscoelastic nonlinear vibrations of imperfect AFG beams", *Appl. Acoust.*, **154**, 121-128. https://doi.org/10.1016/j.apacoust.2019.03.022
Ghayesh, M.H. (2019d), "Dynamical analysis of multilayered cantilevers", *Commun. Nonlinear Sci. Numer. Simul.*, **71**, 244-253. https://doi.org/10.1016/j.cnsns.2018.08.012
Ghayesh, M.H. (2019e), "Nonlinear oscillations of FG cantilevers", *Appl. Acoust.*, **145**, 393-398. https://doi.org/10.1016/j.apacoust.2018.08.014
Ghayesh, M.H. (2019f), "Viscoelastic dynamics of axially FG microbeams", *Int. J. Eng. Sci.*, **135**, 75-85. https://doi.org/10.1016/j.ijengsci.2018.10.005
Ghayesh, M.H. and Amabili, M. (2012), "Nonlinear dynamics of axially moving viscoelastic beams over the buckled state", *Comput. Struct.*, **112**, 406-421. https://doi.org/10.1016/j.compstruc.2012.09.005
Ghayesh, M.H. and Moradian, N. (2011), "Nonlinear dynamic response of axially moving, stretched viscoelastic strings", *Archive Appl. Mech.*, **81**(6), 781-799. https://doi.org/10.1007/s00419-010-0446-3
Ghayesh, M.H., Kazemirad, S. and Darabi, M.A. (2011), "A general solution procedure for vibrations of systems with cubic nonlinearities and nonlinear/time-dependent internal boundary conditions", *J. Sound Vib.*, **330**(22), 5382-5400. https://doi.org/10.1016/j.jsv.2011.06.001
Jouneghani, F.Z., Dimitri, R. and Tornabene, F. (2018), "Structural response of porous FG nanobeams under hygro-thermo-echanical loadings", *Compos. Part B: Eng.*, **152**, 71-78. https://doi.org/10.1016/j.compositesb.2018.06.023
Pegios, I.P. and Hatzigeorgiou, G.D. (2018), "Finite element free and forced vibration analysis of gradient elastic beam structures", *Acta Mechanica*, **229**(12), 4817-4830. https://doi.org/10.1007/s00707-018-2261-9
Ramteke, P.M., Panda, S.K. and Sharma, N. (2019), "Effect of grading pattern and porosity on the eigen characteristics of porous functionally graded structure", *Steel Compos. Struct., Int. J.*, **33**(6), 865-875. http://dx.doi.org/10.12989/scs.2019.33.6.865
Ramteke, P.M., Mahapatra, B.P., Panda, S.K. and Sharma, N. (2020), "Static deflection simulation study of 2D Functionally graded porous structure", *Materials Today: Proceedings*. https://doi.org/10.1016/j.matpr.2020.03.537
Sheng, G.G. and Wang, X. (2019), "Nonlinear forced vibration of functionally graded Timoshenko microbeams with thermal effect and parametric excitation", *Int. J. Mech. Sci.*, **155**, 405-416. https://doi.org/10.1016/j.ijmecsci.2019.03.015
Taati, E. and Fallah, F. (2019), "Exact solution for frequency response of sandwich microbeams with functionally graded cores", *J. Vib. Control*, **25**(19-20), 2641-2655. https://doi.org/10.1177/1077546319864645
Wattanasakulpong, N. and Ungbhakorn, V. (2014), "Linear and nonlinear vibration analysis of elastically restrained ends FGM beams with porosities", *Aerosp. Sci. Technol.*, **32**(1), 111-120. https://doi.org/10.1016/j.ast.2013.12.002
Wu, D., Liu, A., Huang, Y., Huang, Y., Pi, Y. and Gao, W. (2018), "Dynamic analysis of functionally graded porous structures through finite element analysis", *Eng. Struct.*, **165**, 287-301. https://doi.org/10.1016/j.engstruct.2018.03.023
Yang, J., Chen, D. and Kitipornchai, S. (2018), "Buckling and free vibration analyses of functionally graded graphene reinforced porous nanocomposite plates based on Chebyshev-Ritz method", *Compos. Struct.*, **193**, 281-294. https://doi.org/10.1016/j.compstruct.2018.03.090
Zhao, J., Xie, F., Wang, A., Shuai, C., Tang, J. and Wang, Q. (2019), "Vibration behavior of the functionally graded porous (FGP) doubly-curved panels and shells of revolution by using a semi-analytical method", *Compos. Part B: Eng.*, **157**, 219-238. https://doi.org/10.1016/j.compositesb.2018.08.087